Arab J Sci Eng (2016) 41:2285–2294
DOI 10.1007/s13369-015-1887-3

RESEARCH ARTICLE - EARTH SCIENCES

Micro-topographic and Geotechnical Investigations of sandstone Wall on Weathering Progress, Aachen City, Germany, case study

G. M. E. Kamh[1] · **Serdar Koltuk**[2]

Received: 12 November 2014 / Accepted: 6 October 2015 / Published online: 30 October 2015

Abstract Rock's surface micro-topography and geotechnical properties' limits are almost altered, on weathering progress, to a new form(s) and limits, respectively. The quantification of weathering damage for a given rock is of value, e.g., to compute weathering rate, weathering intensity, and rock's durability to weathering processes and to take a decision regarding restoration urgency. The current study aims to examine the variation/constancy of micro-topography and geotechnical properties' limits of the sandstone constituting well-aged wall, at Aachen City, on weathering progress over short duration (7 years of investigation from 2007 to 2014). The micro-erosion meter and Equotip hardness tester are tools used for micro-topographic and rock's surface hardness investigations on one hand, and the mercury intrusion porosimetry has been used for pore size distribution and salt susceptibility investigations on the other hand. These tools are accurate, numerical, comprehensive, easily applicable, and preferable particularly for ancient buildings where sampling is not recommended or prohibited. The wall side under consideration has been selected as its constructional blocks present a wide spectrum of weathering forms as well as rock's surface micro-topography (over 7 years of investigation) through increasing the weathering forms' dimensions and/or creation of new weathering forms. The net result of the current study indicated a noticeable variation in stone's micro-topography on weathering progress particularly for stones' surface with scaling, exfoliation, and a decrease in stone's surface hardness. The critical pore size distribution that has increased rock's susceptibility to weathering particularly by salts has been defined.

Keywords Field investigations · MEM · MIP · EHT · Quantification of rock's weathering

Abbreviations

MEM	Micro-erosion meter
EHT	Equotip hardness tester
MIP	Mercury intrusion porosimetry
PSD	Pore size distribution
Ro.R.S	Roughness range scale
Re.R	Recession range
Ro.C	Roughness class
SSH	Stone surface hardness
RSSH	Relative stone surface hardness
SSI	Salt susceptibility index
A.Ro	Average roughness

1 Introduction

Weathering is the deformation or decomposition of materials through physical and/or chemical processes, respectively. It is acting on all subaerial materials, particularly constructional rocks of a given building, deforming or altering its original topographic and geotechnical (petrophysical and mechanical) properties' limits to a dramatic forms and limits, respectively. Some diagnostic weathering forms can be created at stone's surface characterizing weathering processes, mechanisms and/or intensity that took place even several decades ago. The investigation of weathering progress on

✉ G. M. E. Kamh
gkamh2013@yahoo.com

Serdar Koltuk
koltuk@lih.rwth-aachen.de

[1] Faculty of Science, Menoufiya University, Al Minufiyah Egypt

[2] Department of Engineering Geology and Hydrogeology, RWTH Aachen University, Lochnerstr. 4-20, 52064 Aachen Germany

the constructional materials of a given building is of value to be considered, quantified, and rated particularly before conservation decision is made. [1] is considered as a well-known literature regarding semiquantification of rock's damage categories for a given structure that is based on measuring the weathering forms' dimensions, frequency, and creating intensity scale. This is followed by mapping of these three parameters to finally get the overall rock's damage category using the scheme of damage category including all weathering forms (DCAW Scheme, [2]). The damage category scale that has been constructed [1] for defining the damage category of a given building is listed as follows:

D.C. 0 No visible damage can be observed; D.C. 1 Very slight damage can be observed; D.C. 2 Slight damage can be observed; D.C. 3 Moderate damage can be observed; D.C. 4 Severe damage can be observed; and D.C. 5 Very severe damage can be observed.

The current study has a new target in this regard that can be achieved by tracing the deformation of stone's surface micro-topography and measuring the limits of the sandstone geotechnical properties on weathering progress at natural conditions over 7 years of investigation. Also, it aims to correlate the weathering forms with each of rock's surface roughness, recession range, relative stone's surface hardness, and salt susceptibility index on one hand, and to define the critical pore size that increases the rock's salt susceptibility index on the other hand. This wall has been selected for the current study as it has a considerable variety of weathering forms and intensities; also, it is well exposed to direct daily environmental conditions of solar heating and air humidity (or rainfall) variation. Some fixed points of hard recently made cement-based mortar are standing and taken as a reference points enabling field measurements, particularly by micro-erosion meter, through profiles crossing the building stones' surface with its weathering forms either on 2007 or 2014.

The investigated part of the sandstone wall is located at Latitude 50°45′25″N and Longitudes 6°4′5″ and 6°4′20″E, with total length 200 m and height range 10–25 m above its surrounding ground level (Fig. 1).

The constructional rock of this wall has almost quartz–wacke composition with medium to fine size, moderately sorted, spherical to subspherical quartz grains cemented by kaolinite and iron oxide; K-feldspar is one of the components of this sandstone [3]. Such sandstone type has been selected for the current study, but other blocks with coarse grained, ill sorted, sandstone (constituting the parts of this wall) have been denied to avoid misinterpretation of the results due to varieties in texture or composition of the constructional sandstone of this wall. The weathering damage over 7 years has been investigated for this wall following the detailed field investigation technique of [1,2] to achieve the aims of the current study.

2 Methodology

The following field and laboratory investigations have been conducted to achieve the aims of the current study.

2.1 Field Investigations

2.1.1 Tracing Rock's Surface Micro-topography Using MEM

Several previous literatures had been concerned with measuring rock's surface weathering [4] and the equipment(s)

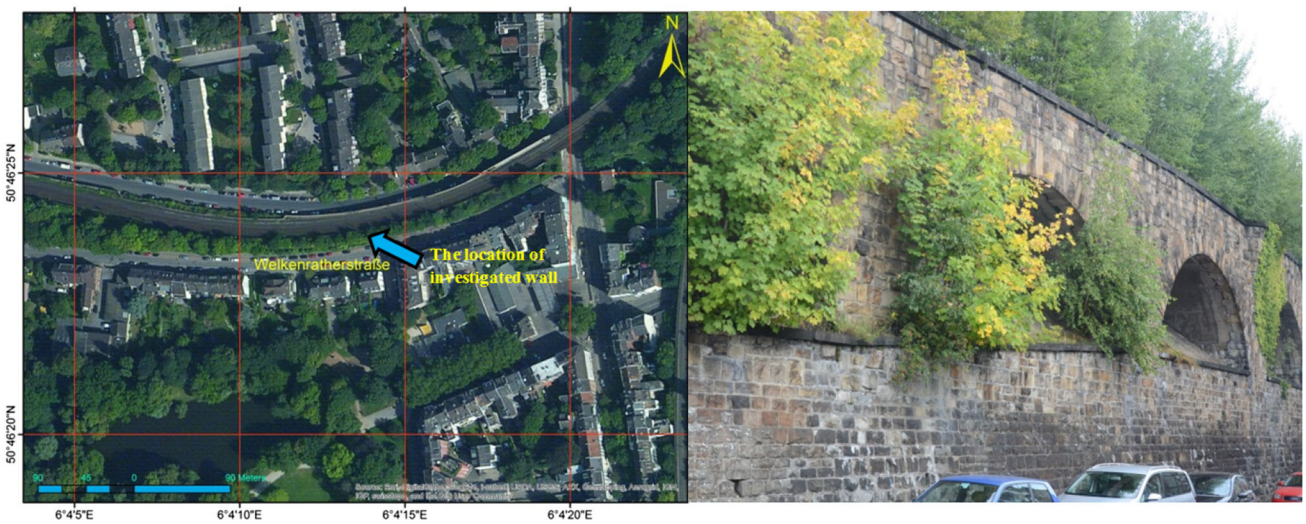

Fig. 1 Location of the study area (*left*) and general view of a part of the investigated wall (*right*)

that can be used for rock's surface hardness [5]. Over two separate periods of investigation (2007 and 2014), the deformation (by weathering) of the sandstone blocks' surface on microscale (for the wall under investigation) has been traced using MEM that has been recorded in previous literatures to be efficient tool for such microscale measurements [6–8]. The MEM used in the current study is composed of 300 thin pen moving forward–backward on a digital ruler enabling tracing all micro-topographic changes at the stone's surface along a profile of 55 cm length with high accuracy of less than 0.1 mm. So, it can be used to draw the micro-topography of the weathered surfaces of the wall under investigation along profiles shown in Fig. 2. The MEM data have been used to create a roughness range scale (Ro.R.S.) and roughness classes (Ro.C.) regarding this wall side (Table 1). The stone's surface irregularities control its weathering susceptibility in the following years where stone's surface with low roughness class is expected to have lower weathering susceptibility than those with higher roughness class [9,10].

The MEM enables us to compute recession range (Re.R) that is defined as the range of differences between the same point on the two roughness profiles of 2007 and 2014. This might reflect weathering regime (uniform or nonuniform) at the constructional blocks of the wall under investigation. The recession range also reflects the equal and/or unequal weathering intensity either due to rock–mortar interaction or heterogeneous durability of the rock under investigation. The rock's surface backward recession is expected to continue till the stability of rock's topography before the recession regime reverses forming a new topographic feature, e.g., the rock with domal form may be reversed to create concave form on weathering progress.

The profiles, on the wall under investigation, for MEM measurements have been selected to cross all detected weathering forms at condition of reference points (recently made hard cement-based mortar) that stands at the two measuring episodes 2007 and 2014; otherwise, the measuring profile is canceled. The weathering forms detected and considered in the current study are as follows: contour scaling, case hardening, granular disintegration into sand, scaled stone margins resulting in domal form, scaling at stones' central part results in concave form, uniform back-weathering "exfoliation," surface partly inhibited by micro-plants, surface partly inhibited by lichens (Fig. 2).

2.1.2 Measuring of Relative Stone's Surface Hardness (RSSH)

The stone's hardness reflects its durability to deterioration by internal and/or external stresses, e.g., salt growth within rock's pores and/or repeated cycles of weathering by natural environmental processes, respectively. Also, the same rock type at each weathering form is expected to have different limits of geotechnical properties particularly hardness; consequently, its durability to weathering processes do. For more explanation, a given rock with case hardening compared with similar rock but with contour scaling is different in their current hardness (durability) as well as to further weathering susceptibility. As rock sampling for hardness measurement is almost prohibited for some buildings and as such measurement (e.g., by Schmidt Hammer) require considerably big-size rock samples in the form of cubes or cylinders [9], and as we are aiming to keep the weathering forms for further investigations, then a simple, accurate, and nondestructive tool named Equotip hardness tester (EHT) has been used in the current study. This is to measure the stone's surface hardness (SSH) at each weathering form, as well as at control (reference) rock surface at this wall side. In turn, this is to compute the RSSH at each weathering form using the equation of [11]:

$$\text{RSSH} = \text{Lt}/\text{Li}$$

where Lt is the stone's surface hardness (SSH) at the weathered part of stone's surface; Li is the stone's surface hardness (SSH) measured at un-weathered (control) stone's surface.

Five measurements of SSH have been taken, to compute their average value, at each of control and weathered parts of this wall.

The measuring points have been selected following the method of [11], i.e., dry, smooth, even surface parts, to avoid any technical errors during measurements taken on August 2014. The interpretation of the resulted RSSH, for the selected parts on this wall, into low, moderate, or high RSSH will be based on the classification (Table 2) listed below.

2.2 Laboratory Investigation

The rock's pore size distribution (PSD) has been reported to be the main culprit behind rock's susceptibility to weathering processes particularly by salts [12–14]. Salt solute influx within rock's pore system (to or at stone's surface) [15] in conjunction with rate of evaporation at stone's surface [16–18] might control the resultant weathering form(s) [19,20]. The PSD has been attributed in previous literatures that rocks with pore radius less than 0.05 μ are highly susceptible to salt weathering [21], while [16] indicated that rock with pore radius less than 0.1μ is highly susceptible to salt weathering, and that with pore radius 0.5 μ is highly susceptible [22,23] and that with pore radius range 0.5–5 μ is highly susceptible [15]. Consequently, there is no specific pore radii for all rock types or salt solutes that ensure high rock's salt weathering susceptibility enables salt weathering reaching its ultimate destructive impact on the host rock.

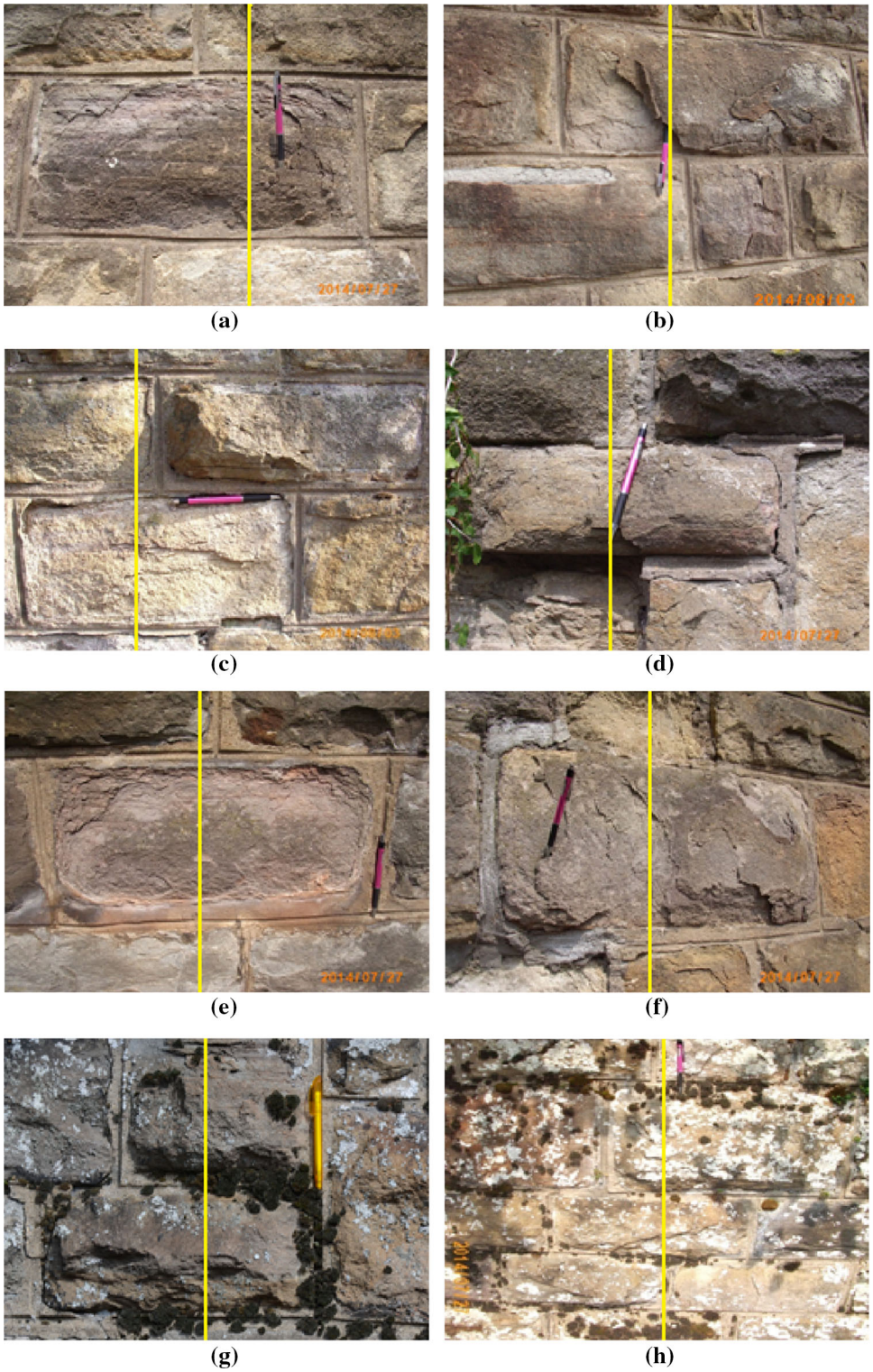

Fig. 2 Weathering forms and profiles considered for MEM measurements across contour scaling (**a**); case hardening (**b**); granular disintegration (**c**); marginal weathering forming domal form (**d**); central weathering forming concave form (**e**); exfoliation (**f**); stone surface covered by micro-plants (**g**); and stone surface covered by Lichens (**h**)

The rock's pore size distribution (PSD) has been examined for two control samples as well as one small sample collected at each of the weathering forms considered in the current study. All samples have been tested using mercury intrusion porosimetry (MIP-5900) at low and high mercury pressure (13000 and 30000 Mpa, respectively) to reach all rock's pore system. Then, the resultant data have been processed to find out the PSD and rock's salt susceptibility index (SSI) for both weathered and control samples. The data processing, SSI classification, and interpretation have been conducted following [18] equation and interpretation (Table 3).

Table 1 Roughness range scale and roughness classes for the MEM data of the sandstone wall, Aachen City

Roughness range scale "Ro.R.S."	Roughness classes "Ro.C."
More than 1.26	Very high roughness
1.12–1.26	High roughness
1.05–1.12	Moderate roughness
1.03–1.05	Low roughness
1.00–1.03	Very low "negligible" roughness

Table 2 Classification of relative stone surface hardness and its interpretation for weathering grade

RSSH range	RSSH class	Interpretation
Less than 0.45	Low	Severely weathered rock
0.45–0.75	Moderate	Moderately weathered rock
More than 0.75	High	Slightly weathered rock

Table 3 SSI classification for the sandstone wall, Aachen City [18]

SSI	Interpretation
$0 \leq \text{SSI} < 1$	Extremely salt-resistant
$1 \leq \text{SSI} < 3$	Very salt-resistant
$3 \leq \text{SSI} < 7$	Salt-resistant
$7 \leq \text{SSI} < 10$	Salt-prone
$10 \leq \text{SSI} < 15$	Very salt-prone
$15 \leq \text{SSI} < 20$	Extremely salt-prone

$$\text{SSI} = \left(I_{\text{pc}} + I_{\text{pm0.1}}\right)\left(P_{\text{m5}}/P_{\text{c}}\right)$$

I_{pc} is index of total connected porosity; $I_{\text{pm0.1}}$ is index of micro-porosity of pores smaller than 0.1 μ in radii; P_{c} is total connected porosity; P_{m5} is micro-porosity of pores smaller than 5 μ in radii.

A correlation between PSD and SSI will be invented to detect the critical pore size that increases rock's susceptibility to salt weathering, i.e., converting the rock from salt-resistant to salt-prone or very salt-prone. This increase in SSI enables higher susceptibility to weathering deforming rock's micro-topography on micro- or mesoscale (quantitatively measured by MEM) and probably reaching to a catastrophic weathering state that requires total reconstruction by freshly quarried dimensional rock.

Based on the inter-relationship between the measurements taken by MIP (PSD and SSI), RSSH, and MEM, the stone's surface micro-topographic deformation in the coming decades might be expected if suitable softwares are used for such extrapolation.

3 Results

3.1 MEM and EHT Results

The backward recession range of rock's surface has been computed along the eight profiles crossing the weathering forms at the wall under investigation (Fig. 2a–h), as the difference between each pair of points of rock's surface roughness over the two periods (2007 and 2014) at this wall side (Fig. 3a–h).

The micro-erosion meter data including roughness (on 2007 and 2014), average roughness, roughness class, and the computed recession range at the eight profiles under consideration are listed in Table 4. These data enable a numerical and graphical detection of weathering progress on the sandstone exposed to such environmental conditions. This can throw light on which weathering form(s) has higher susceptibility to weathering than other forms. Domal form highlights the rock–hydraulic lime mortar interaction represented by salt attack to rocks' margins by salts chemically created on partial alteration of mortar's carbonate content to salts [3,24] by acid rain that is expected to dominate in Europe.

The stone's surface hardness (SSH) has been tested in the current study (August 2014) using EHT as a nondestructive tool concerning the weathering forms under investigation as well as control points (Table 4). Then, the relative stone's surface hardness (RSSH) has been computed by dividing the SSH of the weathered form by the SSH of the control surface. Simply, on weathering progress, the stone's surface hardness decreases on weathering progress creating one or more of weathering forms, but on detachment of these weathering forms, slightly weathered to fresh rock's surface (with higher RSSH) outcrops. The inter-relationship between weathering forms and each of roughness classes and RSSH will be discussed within the scope of this study. The RSSH results listed in table (2) have been graphically plotted in Fig. 4 presenting a classification (low, moderate, and high RSSH) of weathering forms regarding the RSSH of the stone's surface holding these forms.

3.2 MIP Results

The rock's pore properties have been measured for two control samples as well as one sample representative for each of the investigated weathering forms. The results are processed to get the SSI and its interpretation as well as PSD following [18]. The two classifications of PSD used in the current study (that with PSD from <0.01–100 μ and that from <0.05μ up to >5μ where the latter as a detailed sector from the former one for more clarification of the PSD that controls rock's SSI) are of value for more specification of the critical pore radii characterizing salt-resistant rock from salt-prone or down to very salt-prone one (Table 5).

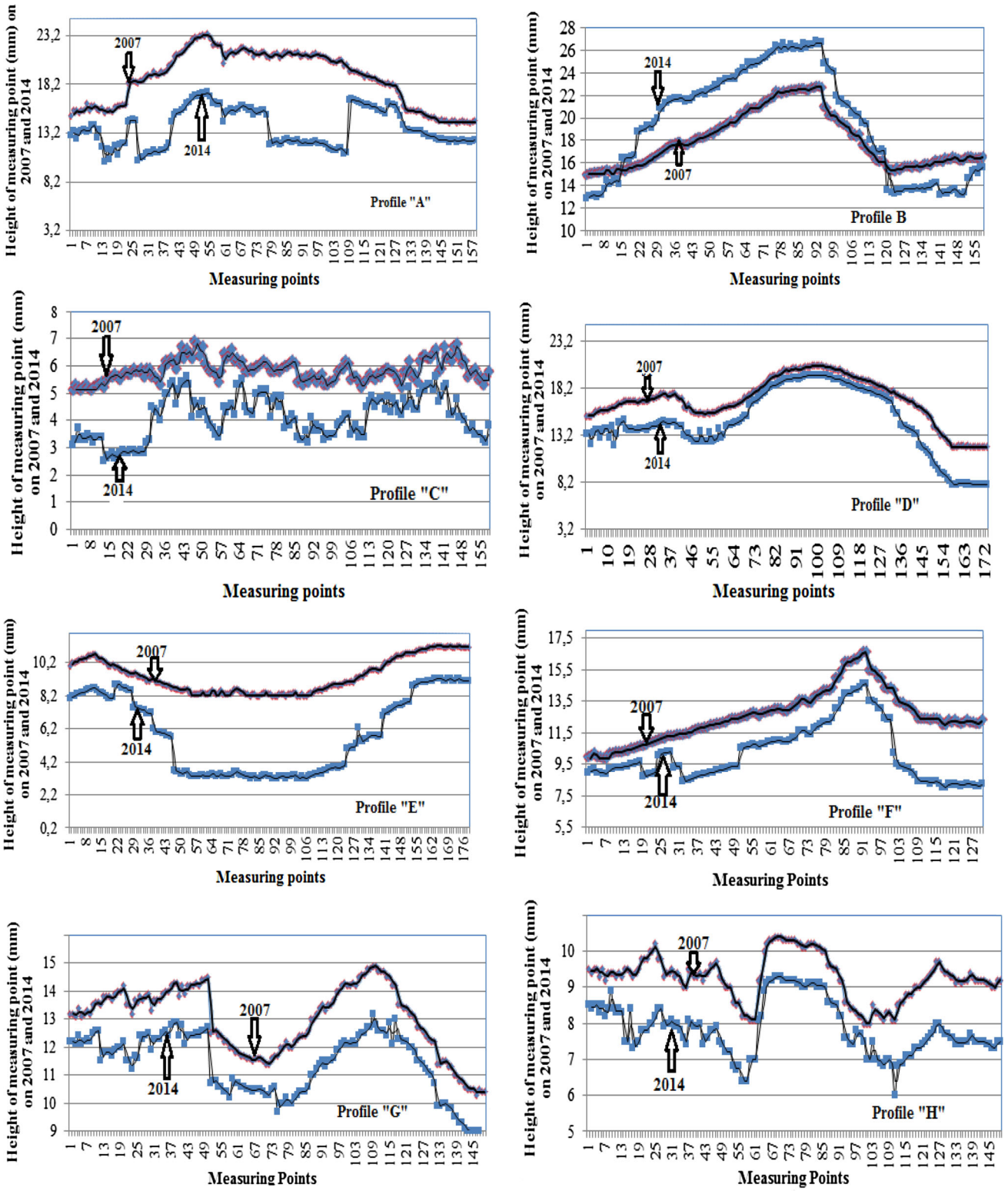

Fig. 3 Graphical representation of rock's surface roughness on 2007 and 2014 along profile *A* crossing contour scaling; profile *B* crossing case hardening; profile *C* crossing granular disintegration into sand; profile *D* crossing domal form; profile *E* crossing concave topography; profile *F* crossing exfoliation; profile *G* crossing rock surface with micro-plants; and profile *H* crossing rock surface with lichens and algae, of constructional sandstone blocks of the wall under investigation, Aachen City

Table 4 Micro-erosion meter and Equotip hardness tester results measured for the eight profiles passing by the weathering forms under consideration, sandstone wall, Aachen City, Germany

Weathering profile	Main weathering forms	MEM results				EHT results	
		Roughness (Ro) in mm (2007–2014)	Average roughness (A.Ro) in mm	Roughness Class (Ro.C)	Recession Range (Re.R) in mm (2014)	Average RSSH	Classes of RSSH
Sandstone wall (*South–Southwest facing wall side*), *Aachen City*							
A	Contour scaling	1.15–1.17	1.16	High	1.8–9.0	0.39	Low
B	Case hardening	1.09–1.00	1.05	Low	−0.30–4.0	0.86	High
C	Granular disintegration	1.09–1.11	1.10	Moderate	0.6–3.0	0.34	Low
D	Domal form	1.31–1.35	1.33	Very high	1.0–4.0	0.63	Moderate
E	Concave form	1.08–1.11	1.10	Moderate	1.1–4.6	1.0	High
F	Exfoliation	1.20–1.23	1.22	High	1.1–4.0	0.36	Low
G	Stone surface covered with micro-plants	1.06–1.20	1.13	High	0.8–2.0	0.73	Moderate
H	Stone surface covered with Lichens	1.07–1.19	1.13	High	0.5–2.0	0.83	High

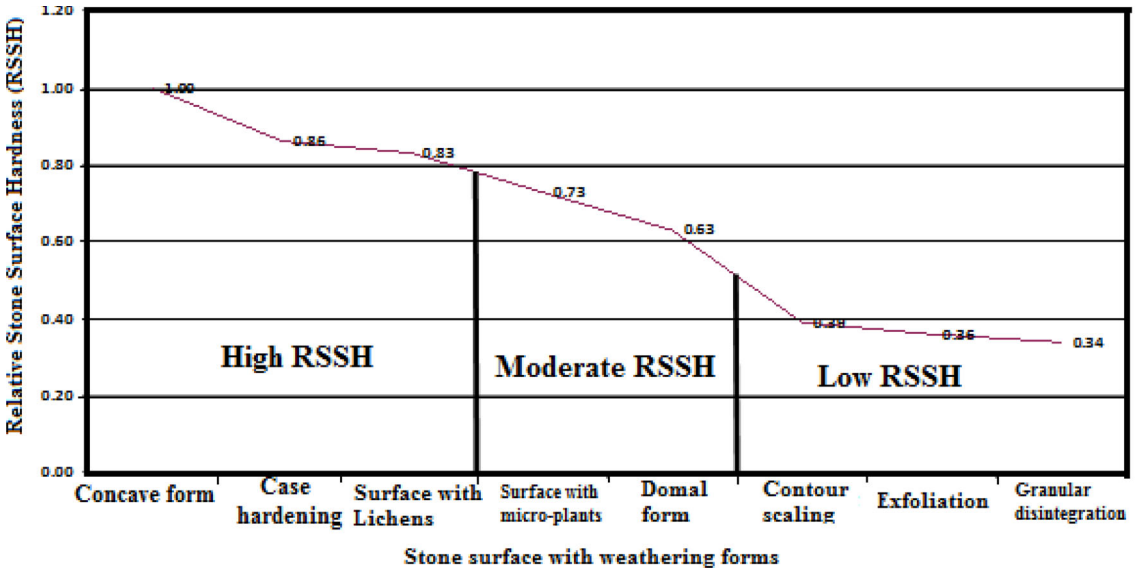

Fig. 4 Graphical representation of relative stone's surface hardness and its classes at the weathering forms under investigation

The outcome of this analysis is to get SSI for ranking the weathering forms based on this parameter as well as to find out the critical PSD that result in increasing rock's SSI, i.e., to be altered from salt-resistant rock to salt-prone or very salt-prone on weathering progress in the coming decades. The inter-relationship between RSSH and SSI classes (Tables 4 and 5) has also been investigated. It indicated an inverse proportional relation with considerably high correlation coefficient (R2 = 0.7327, Fig. 5).

4 Discussion

The investigation of weathering damage for a given structure (e.g., Cathedral, Church, building with unique design or decoration) must be conducted using nondestructive tools or techniques that require tiny size rock samples to avoid more deterioration for the structure. The micro-erosion meter data indicated that the backward recession of stone's surface is variable from one form to the other and even on the same

Table 5 Rock and pore properties for sandstone samples collected at control and weathered forms and examined using MIP-5900, sandstone wall, Aachen City

Sample description	Rock properties						Volume (%) of each pore size distribution "PSD" (<0.01 to 100μ)					Volume (%) of each pore size distribution "PSD" (<0.05 to >5 μ)					
	Total porosity (%)	Bulk density (gm/cm3)	Skeletal density (gm/cm3)	Incremental pore volume "Ipv" (mL/g)	Salt Susceptibility Index (SSI)		<0.01	0.01–0.1	0.1–1	1–10	10–100	<0.05	0.05–0.1	0.1–0.5	0.5–1	1–2.5	2.5–5	>5
					Value	Interpretation												
Control sample 1	14.07	2.23	2.59	0.063	4.47	*Salt-resistant*	8.60	3.51	14.88	68.01	5.00	0.00	9.00	3.20	10.21	39.01	30.10	8.50
Control sample 2	16.12	2.12	2.57	0.075	5.37	*Salt-resistant*	0.00	14.11	17.13	63.01	5.75	0.02	6.21	11.01	15.13	37.00	22.02	8.61
Case hardening	15.88	2.12	2.56	0.074	5.38	*Salt-resistant*	0.00	1.92	12.64	79.77	5.67	0.00	5.33	6.75	9.84	42.11	27.05	8.92
Lichen cover	17.45	2.01	2.53	0.081	5.42	*Salt-resistant*	0.00	5.44	15.21	73.21	6.14	8.55	5.92	5.44	8.90	34.95	27.74	8.50
Micro-plant cover	30.10	1.86	2.66	0.160	8.45	*salt-prone*	0.41	11.27	65.54	20.49	2.29	9.21	6.95	39.11	26.30	6.84	7.94	3.65
Concave form	25.80	1.92	2.46	0.155	9.31	*Salt-prone*	0.51	10.16	67.41	17.20	4.72	6.33	4.86	41.30	28.60	5.11	5.34	8.46
Domal form	25.82	1.56	2.16	1.150	10.29	Very salt-prone	1.37	12.28	69.43	15.27	1.65	5.11	5.78	42.90	32.04	5.25	5.22	3.70
Contour scaling	24.35	2.01	2.09	0.092	15.45	Exceptionally salt-prone	5.70	51.35	30.89	5.17	6.89	5.19	44.14	36.24	3.00	2.91	5.32	3.20
Exfoliation	21.23	2.06	2.13	0.960	13.79	*Very salt-prone*	2.09	54.37	35.89	3.06	4.59	2.06	47.32	36.87	3.11	2.87	6.74	1.03
Granular disintegration	23.11	2.05	2.11	0.782	13.92	*Very salt-prone*	2.18	53.61	32.86	3.02	8.33	3.15	41.43	35.64	4.87	3.54	5.82	5.55

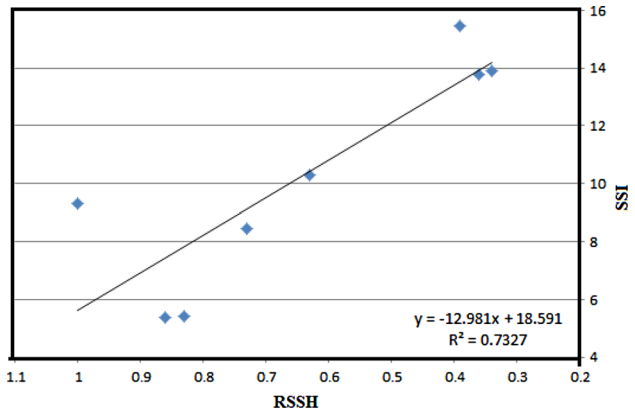

Fig. 5 Relationship between relative stone surface hardness and salt susceptibility index for the sandstone blocks holding the weathering forms under investigation

form but at its different parts (Fig. 3); consequently, it is expressed as a recession range (Re.R) (Table 4). This Re.R can be noted to be unequal with the highest range for constructional sandstone with contour scaling, due to unequal recession at the different parts of this scaling, followed by other weathering forms with high to moderate Re.R. But the sandstone surface with case hardening presents an exceptional case either in A.Ro or Re.R where it does not present backward recession along the whole profile, but at some parts of this profile, the stone's surface, with its consolidating iron oxide leached out from rock's body to its surface by rainfall, protrudes forward resulting in low A.Ro and a negative value of Re.R (Table 4). On weathering progress, this hardened stone's surface will be detached as a whole solid sheet from the rest of the sandstone block holding it. Consequently, an abrupt backward recession of this stone's surface will be formed outcropping a fresh (un-weathered) stone surface ready for further weathering (roughening and recession). Another point that must be addressed is the Ro.C. and Re.R interrelation, the rock's surface with domal topography has very high Ro.C. but with 3mm Re.R compared with Re.R of contour scaling that reaches 7.2mm and high Ro.C. (Table 4). The reason behind that is the A.Ro. is the outcome of dividing the line's length passing across the profile of the form by the straight line between the same two fixed points of measurements. However, the Re.R is the range of minimum and maximum difference between each pair of the same points on the roughness profiles of 2007 and 2014 that seems to be low (due to micro-topographic stability for domal form) compared with contour scaling that still progressing presenting considerably high roughness class with the highest Re.R over these 7 years.

Theoretically, there is an inverse proportional relation between rock's surface roughness and its RSSH class. This is almost correlated with the eight profiles including the weathering forms under investigation but with some exceptions,

e.g., profiles D and H where each has very high and high Ro.C. but still has moderate and high RSSH class (Table 4). The interpretation of that is reaching the stone's surface to the stability state at almost parts of this weathering form (as in profile D) or its cohesion by microorganisms hyphae (as in profile H), consequently, have moderate and high RSSH respectively although they have very high and high roughness class respectively (Table 4).

Salt ingress and hydration (for sulfates) within rock's pores resulted in an alteration of such sandstone from salt-resistant (with PSD 1–5 μ) to almost very salt-prone (with PSD in the range of 0.05–0.5 μ) (Table 5). Correlating the classes of SSI (from salt-resistant down to very salt-prone) with the classes of RSSH (Table 4), clear direct proportional relation can be noted where salt-resistant sandstone has high RSSH; salt-prone sandstone has low to moderate RSSH; and very salt-prone sandstone has almost low RSSH. The variability in SSI of the constructional sandstone of this wall is a result of alteration of its PSD either by filling its pore system with salt crystals or secondary minerals (e.g., iron oxide) leached from rock's inside to or at stone's surface at the prevailing environmental conditions at Aachen City [19,20]. Then, on reaching to PSD of 0.1–1 μ, the salt-resistant sandstone became salt-prone, and on more reduction in pore radii to be almost at the range of 0.05–0.5 μ, it became very salt-prone rock (Table 5). The salts, particularly sulfates [3], started to hydrate (at the humid cold climate dominating in Aachen City) exerting efficient stresses on rock pores' wall as well as along with spread layers at definite depths below stone's surface. These stresses result in fragmentation of rock's components into particles (granular disintegration into sand, [25,26]) or separation of thin sheets (exfoliation and/or scaling, [1]) as noted at this wall (Fig. 2a–h). The results indicated that MEM, MIP, and/or EHT are almost correlated together (Tables 4 and 5) with an exception of concave form that presents high RSSH class, but with PSD resulting in SSI of salt-prone rock, although it is supposed to be salt-resistant rock. This can be interpreted as the surface with moderate roughness class and high RSSH only has pore system filled with salt crystals and/or the leached iron oxide reducing the pores size from salt-resistant range (1–5 microns) to the salt-prone range (0.1–1.0 micron) but still coherent with high RSSH. On repeated salt weathering cycles with this pore system, it is expected to present moderate or low RSSH class particularly at the stone's surface.

5 Conclusion

The current study aimed to examine and define the deformation (weathering and recession) of the micro-topography of the sandstone wall at Aachen City exposed to repeated weathering cycles over 7 years of field investigation using MEM. Not only that but also the alteration in stone's surface hardness at the different weathering forms, created by weathering on this sandstone, using EHT. The susceptibility of this sandstone (particularly each weathering form) to weathering (almost by sulfate salts hydration) has been examined by MIP to detect the PSD. The results indicated that noticeable alteration of rock's surface micro-topography, hardness, and PSD (controlling rock's SSI) has been occurred over this short duration (7 years from 2007 to 2014). The end product of this study can be concluded in the following points: The progress in deformation of rock's micro-topography is noticeably increased or decreased based on the resultant weathering form; the blocks with granular disintegration, exfoliation, and contour scaling have low RSSH, moderate to high roughness class, and are classified as very salt-prone and extremely salt-prone rock surfaces as they have PSD almost in the range of 0.05–0.5 micron. The sandstone surface with domal form and that covered by micro-plants have moderate RSSH, high to very high roughness class, and are classified as very salt-prone and salt-prone rock surfaces with PSD ranging from 0.1 to 1.0 micron. The sandstone surface with concave form, case hardening and that are covered with lichens have high RSSH and are classified as salt-prone and salt-resistant rock surfaces with PSD ranging from 0.1 to 1.0 and 1.0 to 5 micron, respectively.

Acknowledgments The authors are greatly thankful for DAAD for granting this scholarship (for the first author) to conduct this work on WAP program at LIH; RWTH Aachen University, Germany. Also, we are thankful to staff at the main laboratories of RWTH Aachen University to use the equipments required for this work. We appreciate the efforts in English language corrections of this paper done by Prof Dr./ Martin Alex, and the efforts of the AJSE staff for the fruitful comments on this paper.

References

1. Fitzner, B.; Heinrichs, K.; Kownatzki, R.: Weathering forms, classification and mapping/verwitterungsformen–Klassifizierung und Kartierung. Denkmalpflege und Naturwissenschaft, Natursteinkonservierung, V. 1 Berlin Ernst and Sohn, pp. 41–88 (1995).
2. Fitzner, B.; Heinrichs, K. : Damage diagnosis on stone monuments-weathering forms, damage categories and damage indices. In: Prikryl, R.; Viles, H.A. (eds.) Understanding and Managing Stone Decay, pp. 11–56. The Karolinum Press, Prague (2002)
3. Kamh, G.M.E.: Salt weathering, bio-deterioration and rate of weathering of dimensional sandstone in ancient buildings of Aachen City, Germany. Int. J. Water Resour. Environ. Eng. **3**(5), 87–92 (2011)
4. Moses, C.; Robinson, D.; Barlow, J.: Methods for measuring rock surface weathering and erosion: a critical review. Earth Sci. Rev. **135**, 141–161 (2014)
5. Viles, H.; Goudie, A.; Grab, S.; Lallely, J.: The use of the Schmidt hammer and Equotip for rock hardness assessment in geomorphology and heritage science: a comparative analysis. Earth Surf. Process. Landf. **36**(3), 320–333 (2011)

6. Gill, E.D.; Lang, J.G.: Micro-erosion meter measurements of rock wear on the Otway Coast of South-east Australia. Marine Geol. **52**, 141–156 (1983)
7. Stephenson, W.J.; Finlayson, B.L.: Measuring erosion with the micro-erosion meter—contributions to understanding landform evolution. Earth Sci. Rev. **95**, 53–62 (2009)
8. Stephenson, W.J.; Kirk, R.M.; Hemmingsen, S.A.; Hemmingsen, M.A.: Decadal scale Micro-erosion rates on shore platforms. Geomorphology, **114**, 22–29 (2010)
9. Williams, R.B.G.; Robinson, D.A.: The effect of surface texture on the determination of the surface hardness of rock using the Schmidt Hammer. Earth Surf. Process. Landf. **8**, 289–292 (1983)
10. Danny, M.C.; Atle, N.: Rock surface roughness as an indicator of degree of rock surface weathering. Earth Surf. Process. Landf. **21**, 963–977 (1996)
11. Aye, T.; Oguchi, C.T.; Takaya, Y.: Evaluation of sulfate resistance of Portland and high alumina cement mortars using Hardness test. Constr. Build. Mater. **24**, 1020–1026 (2010)
12. Sperling, C.H.B.; Cooke, R.U.: Laboratory simulation of rock weathering by salt crystallization and hydration processes in hot arid environments. Earth Surf. Process. Landf. **10**, 541–555 (1985)
13. Benavente, D.; Cura, G.; Fort, M.A.; Ordonez, S.: Role of pore structure in salt crystallization in unsaturated porous stone. J. Cryst. Growth **260**, 532–544 (2004)
14. Angeli, M.; Bigas, J.P.; Benavente, D.; Menendez, B.; Hebrt, R.; David, C.: Salt crystallization in pores: quantification and estimation of damage. Environ. Geol. **52**(2), 205–213 (2007)
15. Zehnder, K.; Arnold, A.: Crystal growth in salt efflorescence. J. Cryst. Growth **97**, 513–521 (1989)
16. Ordonez, S.; Fort, R.; del Cura, G.: Pore size distribution and the durability of a porous limestone. Q. J. Eng. Geol. **30**, 221–230 (1997)
17. Coussy, O.: Deformation and stress from in-pore drying-indicated crystallization of salt. J. Mech. Phys. Solids **54**, 1517–1547 (2006)
18. Swe, Y.; Oguchi, C.T.: Role of pore size distribution in salt uptake, damage, and predicting salt susceptibility of eight types of Japanese building stones. Eng. Geol. **115**, 226–236 (2010)
19. Goudie, A.S.; Cooke, R.U.: Salt efflorescence and saline lakes: a distributional analysis. Geoforum **15**, 563–582 (1984)
20. Oguchi, C.T.; Matsukura, Y.; Kuchitsu, N.: Environmental and seasonal influence on the spatial distribution of salt efflorescence and weathering on brick Kiln walls. Trans. Jpn. Geomorphol. Union **23**, 335–348 (2002)
21. Steiger, M.: Crystal growth in porous materials- 1: the crystallization pressure of large crystals. J. Cryst. Growth **282**, 455–469 (2005)
22. Punuru, A.R.; Ahad, N.C.; Niraj, P.K.; Gauri, K.L.: Control of porosity on durability of limestone at the Great Sphinx, Egypt. Environ. Geolo. Water Sci. **15**(3), 225–232 (1990)
23. Rossi-Manaresi, R.; Tucci, A.: Pore structure and the disruptive or cementing effect of salt crystallization in various types of stone. Stud. Conserv. **36**, 53–58 (1991)
24. Bamaga, S.O.; Mohamed, A.; Majid, Z.A.: Evaluation of sulfate resistance of mortar containing palm oil fuel ash from different sources. Arab. J. Sci. Eng. **38**(9), 2293–2301 (2013)
25. McGreevy, J.P.: Pore properties of limestones as controls on salt weathering susceptibility: a case study. In: Smith, B.J.; Warke, P.A. (eds.) Processes of Urban Stone Decay, pp. 150–167. Donhead, London (1996)
26. Fitzner, B.; Heinrichs, K.; La Bouchardiere, D.: Damage index for stone monuments. Protection and conservation of the cultural heritage of the Mediterranean Cities. In: Proceedings of the 5th International Symposium on the Conservation of Monuments in the Mediterranean Basin, Sevilla, Spain, 5–8 April 2000, pp. 315–326 (2002)